3rd Micro and Nano Flows Conference
Thessaloniki, Greece, 22-24 August 2011

Numerical optimization of passive chaotic micromixers

Aniruddha Sarkar[1,2], Ariel Narváez[2] and Jens Harting[2,1*]
** Corresponding author: Email: j.harting@tue.nl*
1: Institute for Computational Physics, University of Stuttgart, Pfaffenwaldring 27, D-70569 Stuttgart, Germany
2: Department of Applied Physics, TU Eindhoven, Den Dolech 2, NL-5600MB Eindhoven, The Netherlands
(Dated: May 20, 2011)

Due to the lack of turbulence in micromixers diffusion is the main process contributing to microfluidic mixing. Especially mixing of fluids with low diffusivity is a difficult task. The recently discovered mechanism of "chaotic-advection" enhances the diffusion process by stretching and folding the fluid interfaces in order to provide a larger interface. Certain passive micromixers like the staggered herringbone mixer (SHM) apply this concept and succeed in enhancing the mixing process considerably. The optimization of such micromixers is a time consuming and often expensive process. We demonstrate that the application of the lattice Boltzmann (LB) method to study advection and diffusion processes can be an efficient tool to optimize micromixers. By combining finite time Lyapunov exponents to study chaotic advection and Danckwert's intensity of segregation to study the diffusion, we demonstrate how optimal geometrical parameters for the SHM can be found and how diffusion is improved by the complex flow pattern inside the mixer. The current article provides a review of our results published in [1] together with additional studies on modelling diffusive mixing with the LB method.

I. INTRODUCTION

Microfluidics is an interdisciplinary engineering and science branch which connects physics, chemistry, biology and engineering and has applications in various scientific and industrial areas. Here, we are interested in a common building block for microfluidic systems, namely micromixers. A micromixer is a microfluidic device used for effective mixing of different fluid constituents. A typical example is the integration as important component of chemical and biological sensors [2]. It can be used for mixing of solutions in chemical reactions or to efficiently mix for example a variety of bio-reactants, DNA molecules, enzymes and proteins in portable integrated microsystems with minimum energy consumption [3]. In recent years the demand for highly efficient and reliable micromixers has increased substantially in research and in industry. Therefore, their optimized design has become an important field of research [4].

Due to the small dimensions of micromixers laminar flows are created inside the channels causing the mixing performance to be limited. Experiments on channels with complex surface topology have revealed that microscale mixing is enhanced by "chaotic advection", a process which was first reviewed by Aref in 1984 [5]. He describes how mixing is still possible even at low Reynolds number by repeated stretching and folding of fluid elements. If properly applied, this mechanism causes the interfacial area between the fluids to increase exponentially, which can then lead to an enhanced inter-material transport [6]. In a multicomponent system, i.e. a mixture of multiple miscible fluids, the advection process is accompanied by diffusion which is responsible for the mass transport in the mixing process. The diffusivity determines the rate of mixing among different fluids. One needs to carefully study the underlying principles of advection and diffusion in order to understand the mixing process. Our aim is to study these phenomena and develop tools to quantify micromixing. So far most of the numerical research in this area has either been performed only in two dimensions or was restricted to single phase/single component systems. For the applicability to experiments it is, however, highly desirable to study mixing in a three dimensional framework including a fully resolved multiphase/multicomponent description.

The efficiency of a micromixer is often quantified on the basis of its mixing length and mixing time. These are defined as the distance and time span the fluid constituents have to flow inside the mixer in order to obtain a homogeneous mixture. An effective micromixer should reduce the mixing length and time substantially in order to achieve rapid mixing. Efficient mixing is achieved by enhancing the advection and diffusion processes in the micromixers. A common practice to achieve this goal is to design passive devices that create alternating thin fluid lamellae. These result in an interfacial area that increases linearly with the number of lamellae rendering the diffusion process more effective and hence allowing faster mixing [7]. The drawback of such devices is that the number of lamellae is generally limited due to the negative impact on the applied pressure drop caused by the microstructures inside the channel. A so-called "chaotic micromixer" can overcome this drawback to some extend. Such a device consists of microstructured objects such as "herringbones", placed inside a microchannel. The staggered herringbone mixer (SHM) shown in Fig. 1 is the first chaotic micromixer that can be found in the literature. It was developed in 2002 by Stroock et al. [8]. The half cycles of the SHM consist of grooves with two arms which are asymmetric and unequal in length. These arms are inclined at an angle of 45° and the pattern in-

terchanges every half cycle of the mixer. The peculiar arrangement of the herringbone structure enhances the mixing process by "chaotic advection" where the interfacial area between the fluids grows exponentially in time – the most important advantage over mixers using the concept of multi-lamellation.

To compare different micromixers and to improve their design, it is important to develop schemes to quantify their performance. Efficiency and mixing quality have been studied by various methods in the past. These include the analysis of the probability density function of the flow profiles, studying the stretching of the flow field, the Poincaré section analysis. Here, an alternative numerical optimization procedure is presented which is tailored for the optimization of chaotic micromixers and which relies on the advection properties of mixers like the SHM. It is based on lattice Boltzmann (LB) simulations to describe the flow inside complex mixer geometries together with a measurement of finite time Lyapunov exponents (FTLE) as obtained from trajectories of massless tracer particles immersed in the flow. Fig. 2 depicts two typical snapshots from our simulations. The left figure shows a snapshot of the tracer positions just after the start of the simulations. Towards the end of the simulation all tracer particles are homogeneously distributed throughout the mixer demonstrating that the system is fully mixed (right figure). The Lyapunov exponent provides a quantitative measure of long term average growth rates of small initial flow perturbations and thus allows a quantification of the efficiency of chaotic transport [9, 10]. We apply Wolf's method to calculate the FTLE since the systems of interest are finite and simulations are limited to a finite time span [7]. We can compute the mixing length of various mixers based on the intensity of segregation (I_d) as introduced by Danckwerts in 1952 [6, 11]. Both numerical schemes have the potential to assist experimental optimization since geometrical parameters or fluid properties can easily be changed without requiring a new experiment. To demonstrate its applicability, the FTLE technique is applied to evaluate the optimal parameters of the SHM based on single component flows. The concentration profiles of the fluids obtained from the multicomponent LB simulations are used to estimate I_d, which can then be used to evaluate the mixing length for mixcromixers.

II. SIMULATION METHOD

II.1. Single component fluid – advection analysis

For a description of the fluid flow inside the micromixer, we apply the lattice Boltzmann method (LBM), a simplified approach to solve the Boltzmann equation in discrete space, time and with a limited set of discrete velocities [12]. The Boltzmann equation, given as

$$\partial_t f + \mathbf{c} \cdot \nabla f = \Omega(f), \tag{1}$$

describes the evolution of the velocity distribution function by molecular transport and binary intermolecular collisions. $f(\mathbf{r}, \mathbf{c}, t)$ represents the distribution of velocities in continuous position and velocity space, $\mathbf{r}$ and $\mathbf{c}$, respectively. The position $\mathbf{x}$ at which $f(\mathbf{x}, \mathbf{c}_k, t)$ is defined, is restricted to a discrete set of points on a regular discrete lattice with lattice constant Δx. The velocity is restricted to a set of velocities $\mathbf{c}_k$ implying that velocity is discretized along specific directions. Δt denotes the discrete time step. The model we adopt is a D3Q19 model, i.e. a 3D model with 19 different velocity directions [13]. The right hand side of the above equation represents the collision operator which is simplified to a discretized linear Bhatnagar-Gross-Krook (BGK) form [14] that can be written as

$$\Omega_k = -\frac{1}{\tau}(f_k(\mathbf{x}, t) - f_k^{\mathrm{eq}}(\mathbf{x}, t)). \tag{2}$$

Here, τ is the relaxation time of the system, which controls the relaxation towards the Maxwell-Boltzmann equilibrium distribution $f_k^{\mathrm{eq}}(\mathbf{x}, t)$. By considering small velocities and constant temperature, a discretized second order Taylor expansion of the above equilibrium distribution function can be written as

$$f_k^{\mathrm{eq}}(\mathbf{x}, t) = \zeta_k \frac{\rho}{\rho_0} \left(1 + \frac{\mathbf{c}_k \cdot \mathbf{u}^{\mathrm{eq}}}{{c_s}^2} + \frac{(\mathbf{c}_k \cdot \mathbf{u}^{\mathrm{eq}})^2}{2{c_s}^4} - \frac{\mathbf{u}^{\mathrm{eq}} \cdot \mathbf{u}^{\mathrm{eq}}}{2{c_s}^2}\right), \tag{3}$$

where ζ_k are the lattice weights, ρ is the density, ρ_0 a reference density, and $c_s = (1/\sqrt{3})\Delta x/\Delta t$ is the speed of sound. $\mathbf{u}^{\mathrm{eq}}$ is the equilibrium velocity of the fluid, which is shifted from the mean velocity by an amount $\tau\mathbf{g}$ under the influence of a constant acceleration $\mathbf{g}$. The evolution of the LB process takes place in two steps: the collision step where the velocities are redistributed along the directions of the lattice and the propagation step by which they are displaced along these directions. This leads to the discretized Boltzmann kinetic equation:

$$f_k(\mathbf{x}+\Delta t\mathbf{c}_k, t+\Delta t) - f_k(\mathbf{x}, t) = -\frac{\Delta t}{\tau}(f_k(\mathbf{x}, t) - f_k^{\mathrm{eq}}(\mathbf{x}, t)). \tag{4}$$

Here, the macroscopic fluid density is given by

$$\rho(\mathbf{x}, t) = \rho_0 \sum_k f_k(\mathbf{x}, t) \tag{5}$$

and the macroscopic fluid velocity in the presence of external forcing is given by

$$\mathbf{u}(\mathbf{x}, t) = \frac{\rho_0}{\rho(\mathbf{x}, t)} \sum_k f_k(\mathbf{x}, t)\mathbf{c}_k - \frac{\Delta t}{2}\mathbf{g}. \tag{6}$$

It can be shown by a Chapman-Enskog expansion that the macroscopic fields $\mathbf{u}$ and ρ from the above equations fulfill the Navier Stokes equation in the low Mach number

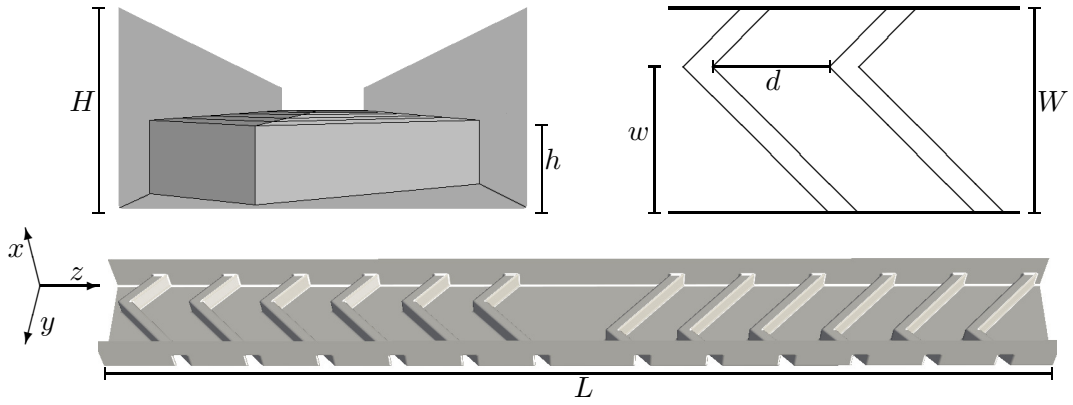

FIG. 1. A typical example of a SHM geometry as it is used for the simulations. The dimensions of this channel are $32\times64\times L/\Delta x$ lattice units, where L depends on the distance between the grooves d and the number of grooves per half cycle n. H is the height of the channel, h is the height of the grooves and w denotes the horizontal length of the long arm. We define the height fraction as $\alpha = h/H$, width fraction as $\beta = w/W$, and the distance fraction as $\gamma = d/L$. The top boundary at $x = 32$ is not shown in the figure (from [1]).

limit and for isothermal systems [12]. In order to simulate a fluid flow through microchannels, periodic boundary conditions are implemented along the flow direction (see Fig. 1) and no-slip bounce back boundary conditions are imposed at the channel walls.

We simulate a fluid flowing inside a SHM with a cross section of $96\mu\text{m} \times 192\mu\text{m}$. The length of the mixer is of the order of 1536μm, but can be varied in order to always accommodate a full cycle of the herringbone structure. For computational efficiency we have chosen a lattice resolution of $\Delta x = 3\mu$m. In the LB method, the kinematic viscosity is related to the discrete time step through the expression $\nu = {c_s}^2\Delta t\,(\tau/\Delta t - 1/2)$. $\tau/\Delta t$ is chosen to be 1 and the simulated fluid has the kinematic viscosity of water, $\nu = 10^{-6}\text{m}^2\text{s}^{-1}$. This implies for the current choice of Δx that $\Delta t = 1.5\mu$s and $c_s = 1.15$m/s. The Reynolds number $\text{Re} = u\,\ell/\nu$ of the flow is ≈ 1.3, where $\ell = \sqrt{H^2 + W^2}$ is the characteristic length of the channel. H denotes the height of the channel and W denotes the width of the channel. One set of simulations is obtained for g being $0.4 \times 10^{-3}\text{m/s}^2$ which corresponds to $\text{Re} \approx 0.4$.

Trajectories of massless and non-interacting tracer particles introduced into the flow are obtained by integrating the vector equation of motion

$$\frac{\mathrm{d}\mathbf{R}_j}{\mathrm{d}t} = \mathbf{u}(\mathbf{R}_j), \quad j = 1, ..., P, \tag{7}$$

where $\mathbf{R}_j$ denotes the position vector of an individual tracer particle. The velocity $\mathbf{u}(\mathbf{R}_j)$ is obtained from the discrete LB velocity field through a trilinear interpolation scheme. After the flow simulation has reached its steady state, $P = 1000$ particles are introduced at fluid nodes in the inlet and then their velocities are integrated at each time step.

A general feature of chaotic systems is that two nearby trajectories diverge exponentially in time. The rate of divergence can be related to the strength of the flow field to create conditions for chaotic mixing. The Lyapunov exponent is a possible measure for this effect and is defined as

$$\lambda_\infty = \lim_{t\to\infty} \frac{1}{t} \ln \frac{\mathcal{D}(t)}{\mathcal{D}(0)}, \tag{8}$$

where $\mathcal{D}(t)$ is the distance between two trajectories at time t. Since any real system is finite it is not possible to implement this definition to quantify mixing. Also, when two trajectories separate from each other, this definition does not allow to understand the ongoing stretching and folding dynamics. A quantitative measure of mixing based on the Lyapunov exponent can be obtained by using the FTLE instead [15, 16]. It is defined as [17]

$$\lambda_{\text{FTLE}} = \frac{1}{\delta t} \ln \frac{\mathcal{D}(t + \delta t)}{\mathcal{D}(t)}, \tag{9}$$

where t is any particular instant of time and δt is a finite time after which the FTLE is measured. The same process is repeated over N times. For large N the average FTLE converges to the Lyapunov exponent [16],

$$\lim_{N\to\infty} \langle\lambda_{\text{FTLE}}\rangle_N = \lambda_\infty. \tag{10}$$

Wolf et al. suggested a method to calculate the FTLE from a set of experimental data [7, 18]. Following Wolf's approach, we implement the following equation to quantify the mixer performance on the basis of the average FTLE as

$$\langle\lambda\rangle_N = \frac{1}{N} \sum_{i=0}^{N-1} \frac{1}{\tau_i} \ln \frac{\mathcal{D}(t_i + \tau_i)}{\mathcal{D}(t_i)}, \tag{11}$$

where t_i is the ith time when a FTLE is evaluated, $\mathcal{D}(t_i + \tau_i)$ and $\mathcal{D}(t_i)$ are the distance at time step $t_i + \tau_i$ and t_i, respectively. τ_i is a multiple of Δt and N is

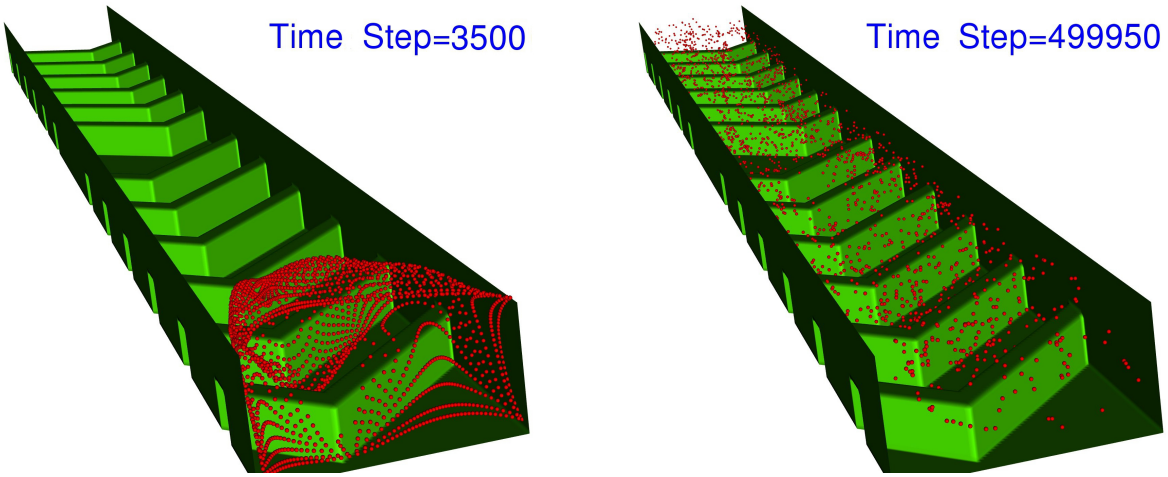

FIG. 2. A snapshot from a typical simulation of flow inside a staggered herringbone micromixer demonstrating the highly regular arrangement of tracer particles at the beginning of the simulation (left) and a fully mixed state at a late stage of the simulation (right). The fluid itself is not shown.

the total number of times the particle positions are re-adjusted. If $\langle\lambda\rangle_N$ has a positive and non-zero value the distance between two nearby particles diverges at an exponential rate. Particle pairs which are initially placed very close to each other are chosen to evaluate the FTLE i.e. with a distance Δx. If the separation is greater than a maximum distance which is half the minimum dimension of the system $H/2$, the distance between the particles is re-adjusted to the initial distance Δx and one of the particles is placed along the line of separation in order to avoid errors due to orientation. If a replacement point cannot be found due to a wall node present at the location, a nearby fluid node is selected instead. If even such points cannot be found, the replacement is postponed to a later timestep. In the implementation of the scheme, for every particle pair one of the trajectories is chosen as the fiducial path, while the position of the other particle is replaced if the distance exceeds the threshold.

II.2. Multi component fluid – diffusion analysis

To simulate the diffusion process involving multiple species with the LB method, we apply a multicomponent fluid solver based on the model by Shan and Chen as an extension to the previously introduced single component LBM [19]. We restrict the explanation of this model to a binary system. The interaction of components A and B is given by a mean field force

$$\mathbf{F}_{AB}(\mathbf{x},t) = -\psi_A(\mathbf{x})G_{AB}\sum_k \zeta_k\psi_B(\mathbf{x}+\Delta t\mathbf{c}_k)\mathbf{c}_k, \quad (12)$$

which depends on the local fluid density and the density of the nearest neighbour lattice sites through an effective mass function $\psi(\mathbf{x},\rho)$ [19]. G_{AB} is the parameter that controls the repulsion between the components and it is symmetric i.e. $G_{AB} = G_{BA}$. While low values of G_{AB} cause the fluids to be miscible, larger values allow the simulation of immiscible fluids. The force $\mathbf{F}_{AB}$ enters Eq. (3) as a shift of the equilibrium velocity $\mathbf{u}^{\mathrm{eq}}$. The macroscopic velocity for component A is then expressed as

$$\begin{aligned}\mathbf{u}_A(\mathbf{x},t) =& \frac{\rho_0}{\rho_A(\mathbf{x},t)}\sum_k f_k^A(\mathbf{x},t)\mathbf{c}_k - \\ &- \frac{\tau_A}{2\rho_A(\mathbf{x},t)}\mathbf{F}_{AB}(\mathbf{x},t) - \frac{\Delta t}{2}\mathbf{g},\end{aligned} \quad (13)$$

where ρ_A, τ_A and f_k^A are the density, the relaxation time, and the distribution function for component A. Similarly we can calculate the velocity for component B. Both components individually satisfy Eq. (4). With the increase in G_{AB} the repulsion between the individual components increases. We use the multi component LB method to simulate typical micromixing experiments. This requires us to investigate a suitable Reynolds and Péclet number (Pé $= u\ell/D_{AB}$) regime. The ratio of Pé to Re is called the Schmidt number (Sc $= \nu/D_{AB}$). The diffusion in a multi component system is governed by Fick's laws. Considering a binary system of components A and B with diffusivity D_{AB} Fick's first law of mass flux of component A into B is

$$\mathbf{j}_A = \rho_A(\mathbf{u}_A - \mathbf{u}) = -\rho D_{AB}\nabla\omega_A, \quad (14)$$

where $\mathbf{u}_A$ is the velocity of component A relative to the mean velocity of the mixture $\mathbf{u}$, ω_A is the mass fraction of A and ρ is the total density. A similar equation can be written for the species B, where $D_{BA} = D_{AB}$. Thus for a binary system we have only one value of diffusivity. After inserting the Fick's first law from Eq. (14) into the continuity equation for the components, we obtain an equation which is known as Fick's second law for diffusion. At a constant temperature and pressure, which

assures a constant ρD_{AB}, Fick's second law is given by

$$\frac{\partial \omega_A}{\partial t} + \mathbf{u} \cdot \nabla \omega_A = D_{AB} \nabla^2 \omega_A. \tag{15}$$

By analyzing the temporal and spatial variation of the concentration field obtained from the multi component LB method and evaluating the derivatives from Eq. (15) we can estimate the diffusivity of the components which we simulate. A measure for the quality of mixing in a micromixer can also be obtained from the concentration field. Danckwerts segregation of intensity (I_d) is used to quantitatively evaluate the performance of different mixing states of micromixers [20]. To evaluate the I_d we need to have knowledge of the concentration field of the system at different locations along the length of the micromixer. Considering the flow to be along the z direction, intensity of segregation is defined as

$$I_d(z) = \frac{\sigma^2(z)}{\sigma^2_{\max}(z)}, \tag{16}$$

where $\sigma^2(z)$ is the standard deviation of the concentration at some plane z inside the channel and

$$\sigma^2_{\max}(z) = c_{\mathrm{mean}}(z)(c_{\max}(z) - c_{\mathrm{mean}}(z)). \tag{17}$$

$c(z)$ is the concentration at a fluid element at position z. $c_{\max}(z)$ and $c_{\mathrm{mean}}(z))$ are the maximum and mean concentration at position z, respectively. The mixing length (Λ) is defined as the value of z when I_d is less than 0.5% of its initial value.

In order to measure I_d in a microchannel, the system is initialized with two parallel fluid lamellae consisting of component A and B. While for the single component simulations periodic boundary conditions were applied in z direction, here we use a so-called recoloring scheme. After leaving the channel at the end and when reentering it at $z = 0$, the ratio of components A and B is redistributed as such that we obtain a constant inflow of two lamellae consisting only of a single component each. Further, the fluid-surface boundary conditions are adopted by a modified Shan-Chen forcing term so that a contact angle of 90 degrees is assured.

III. RESULTS

We study the interplay of advection and diffusion phenomena in micromixers. The first part of this section is based on our single component LB simulations, where we evaluate the optimal parameters of the SHM to create chaotic advection in the flow. The second part is based on multi component LB simulations, where we study mixing of multiple fluids and quantify the mixing length of micromixers based on the diffusive properties.

III.1. Single component fluid – advection analysis

Here we follow our work presented in [1] to demonstrate how FTLE can be utilized for an optimization strategy for chaotic micromixers. The influence of different parameters which directly affect the performance of the SHM is evaluated. These are the ratio of height of the grooves to the height of the channel α, the ratio of the horizontal length of the long arm to the channel width β, the ratio of distance between the grooves to the length of the channel γ and the number of grooves per half cycle n. While keeping all other parameters fixed, the width fraction (β) is varied within the range of 0.22 and 0.82 and the distance fraction (γ) from 0.04 to 0.11. The width of the grooves is kept fixed at 24μm for all simulations. Then, the number of grooves per half cycle (n) is varied from 2 to 10 and the height fraction (α) from 0.125 to 0.343. One has to take care of a thorough convergence of the simulations since $\langle\lambda\rangle_N$ fluctuates before finally converging to a particular value after $\sim 6 \times 10^5$ time steps. The effect of the geometry can be measured by comparing the average of the converged FTLE which is denoted by λ. The error bars in Figs. 3 A to D are given by the standard deviation of the data from the point where it has converged.

Fig. 3 A depicts the variance of λ and as such the performance of the SHM with respect to β for two different Reynolds numbers, Re = 0.4 and 1.3. Due to the symmetry of the mixer geometry, only values for $\beta \geq 0.5$ are plotted. The datasets peak at $\beta = 2/3$ implying that the degree of chaotic advection is maximized for this particular value of the width fraction β. The measurements at different Reynolds numbers depict that changing the driving force does change the absolute value of λ, but has no influence on the general shape of the curve. This is confirmed by similar studies of the Re dependence for other geometrical parameters and various different driving forces. Therefore, we restrict ourselves to Re = 1.3 for all further simulations. Our findings are consistent with the original experimental work of Stroock et al. [8] as well as numerical optimizations by Stroock and McGraw [21]. Both publications show that $\beta = 2/3$ generates a maximum swirling motion of the fluid trajectories. However such analysis with dyes or concentration profiles does not allow to obtain an insight into the behavior of the flow field, while the FTLE does.

In Fig. 3 B, data from a set of simulations with β fixed at the optimized value of 2/3 and the distance fraction γ being varied from 0.04 to 0.11 is shown. It can be observed that after a moderate increase of λ with γ, the curve has a sharp peak at $\gamma = 0.07$, for the current choice of Δx. Afterwards, λ decreases in a similar fashion as for small γ, but still at higher absolute values.

In the following the number of grooves per half-cycle n is varied from 2 to 10. It can be understood from Fig. 3 C that a variation of n has the largest impact on the performance of the mixer as compared to β or γ. For the current setup, by variation of n it is possible to

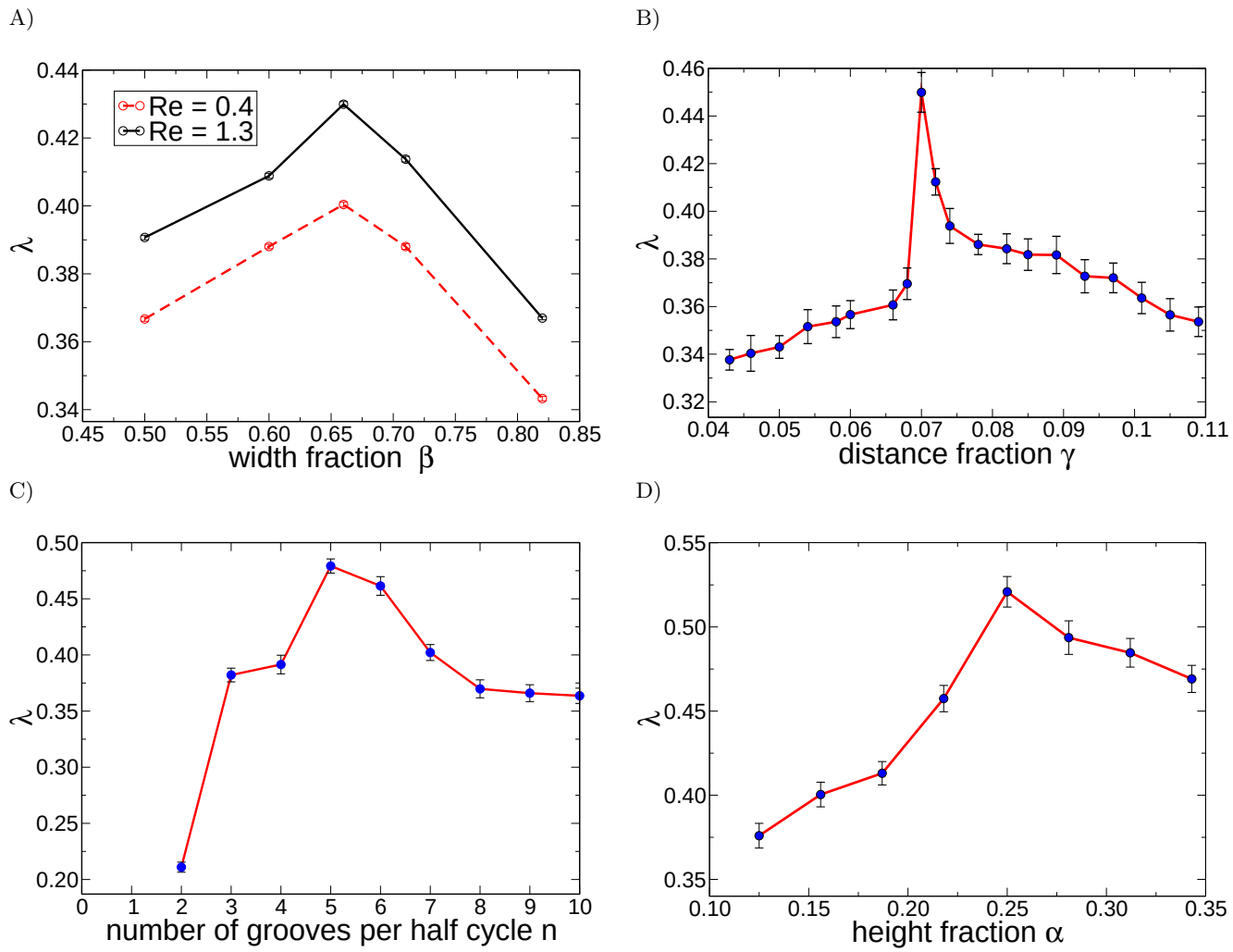

FIG. 3. A) A maximum of the variation of the averaged finite time Lyapunov exponent λ with different width fraction β can be obtained for a width fraction of $\beta = 2/3$. While the position of the maximum is not affected by changing Re, the absolute values do change. B) The FTLE rises with the increase of the distance fraction γ until it reaches a distinct peak. Then, the curve decreases demonstrating an optimized performance of the mixer at $\gamma = 0.07$. C) A maximum of the variation of the maximum averaged finite time Lyapunov exponent λ with different width fraction β can be obtained for a width fraction of $\beta = 2/3$. While the position of the maximum is not affected by changing Re, the absolute values do change. D) The FTLE rises with the increase of the distance fraction γ it reaches a distinct peak. Then, the curve decreases demonstrating an optimized performance of the mixer at $\gamma = 0.07$ [1].

increase the value of λ by a factor of 2.3 as compared to 1.2 for β and 1.3 for γ. The data clearly demonstrates that a staggered herringbone mixer with $n = 5$ performs best.

The final parameter to be considered is the ratio of the half depth of the grooves to the height of the channel α. Fig. 3 D depicts the average value of the converged Lyapunov exponents for α between 0.125 and 0.343. After a strong increase of the curve the data has a maximum at $\alpha = 0.25$. For larger α the value of λ decreases again. Our result are confirmed by the original experimental analysis of Stroock et al. [8].

III.2. Multi component fluid – diffusion analysis

In the section introducing the simulation method it is described how the parameter G_{AB} controls the repulsion between the components. We expect the diffusivity between the components to decrease with the increase of G_{AB}. To estimate the value of D_{AB} we simulate a periodic system with dimensions $1 \times 1 \times 64$. The one dimensional system consists of two lamellae of different components each which are 32Δx long. The fluid densities are initialised as 0.5 in lattice units. By studying the concentration profiles and evaluating D_{AB} from Eq. (15) we find that D_{AB} decreases linearly with G_{AB} (see upper inset of Fig. 4). Our data agrees well with the observa-

tion of Shan and Doolen [22]. G_{AB} has a critical value beyond which the fluids become immiscible. From our tests we obtain a critical value of $G_{AB} = 2.894\ (\rho_0 \Delta t)^{-1}$. We estimate the value of D_{AB} at the critical value of G_{AB} to be $10^{-3}\ (\Delta x)^2/\Delta t$ and use this value of diffusivity for the simulations presented below. To compare different mixers we need to estimate the different mixing lengths Λ. We define Λ at the position where I_d goes below 0.5 % of its initial value. I_d is estimated from the concentration profiles of the system in steady state. The influence of the diffusivity on the mixing length can be observed in Fig. 4 (bottom), where we demonstrate a strongly non linear behaviour showing a saturation.of the mixing length for lagrer values of the diffusivity.

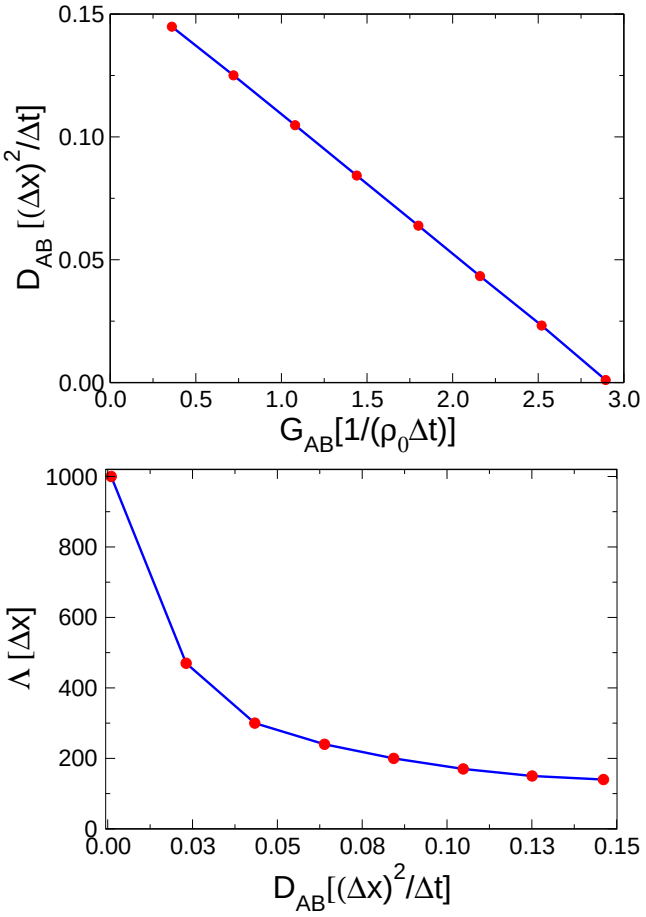

FIG. 4. Top: The diffusivity decreases linearly with the increase of G_{AB}. Bottom: The mixing length Λ is computed from the concentration field and decreases with the increase of D_{AB}.

We can infer that weakly diffusive fluids need a very long channel to show perfect mixing. We simulate flow in two systems, one being a SHM with the optimized parameters obtained from our single component simulations and the other one being a plain channel. Each system is of dimensions 32×64×1546 Δx. From Fig. 5 we can estimate the mixing length for the SHM as $\Lambda_{\mathrm{SHM}} = 493\ \Delta x$ and for the plain channel we obtain $\Lambda_{\mathrm{Plain}} = 782\ \Delta x$

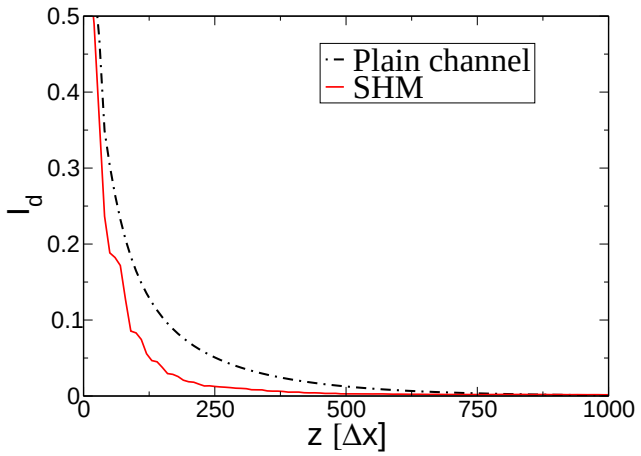

FIG. 5. The measured I_d decreases faster for the SHM as compared to the plain channel indicating that the mixing length decreases by 37% when "chaotic-advection" is introduced into the flow.

corresponding to a 37% reduction in the mixing length when chaotic advection is introduced into the flow [8]. From the experiments on SHM, it can be observed that the difference of mixing lengths becomes more prominent when the diffusivities of the components are lower.

In the plain channel the flow is diffusion dominated. Hence from our preliminary results obtained with the multi component model we can confirm that "chaotic advection" reduces the mixing length by enhancing the diffusion process and evaluating I_d can be used as a tool to quantify the mixing length of micromixers. The challenge which we face is to simulate the experimental set up of Stroock et al. with this multi component model. So far we could achieve $D_{AB} \sim 10^{-3}\ (\Delta x)^2/\Delta t$ which gives Sc $\sim 10^2$. To simulate the experiment, we would need to achieve Sc $\sim 10^7$. Improvements of the simulation model are required to achieve a low diffusivity which can give such high Sc numbers. However, this limitation does not influence the possibility to understand the general interplay between advection and diffusion and use the simulation paradigm presented here as a tool to optimize micromixer geometries.

IV. SUMMARY

Passive chaotic micromixers can be successfully applied to improve mixing at the microscale where turbulence is absent. The processes of advection and diffusion play an important role in determining the efficiency of a micromixer. Micromixing is made more efficient by introducing "chaotic advection" to the flow. Chaotic mixers provide a large fluid-fluid interface by repeatedly stretching and folding of these interfaces. In this work we have demonstrated efficient numerical schemes which allow the quantification of "chaotic advection" and "diffusion" and thus the performance of a micromixer. The first scheme

is based on multi component LB simulations to describe the time dependent flow field in complex mixer geometries combined with Wolf's method to compute FTLE from passive tracer trajectories and I_d from concentration profiles. We have demonstrated the applicability of the quantification methods by applying it to optimize the geometry of the SHM and estimating the mixing length. By performing a systematic variation of the relevant geometrical parameters we obtained a set of optimal values $\alpha = 0.25$, $\beta = 2/3$, $\gamma = 0.07$ and $n = 5$ which is consistent with literature data published by others. An important feature of the method presented here is that it allows optimization of the mixing performance by direct investigation of the underlying dynamical process [1]. Second, we apply multi component LB simulations in order to study the mixing of multi component flows in microchannels. We can estimate the diffusivity based on Fick's diffusion laws and estimate the mixing length by studying the spatial variation of the steady state concentration field.

V. ACKNOWLEDGMENTS

This work was financed within the DFG priority program "nano- and microfluidics", the DFG collaborative research center 716, and by the NWO/STW VIDI grant of J. Harting. We thank the Scientific Supercomputing Center Karlsruhe and the Jülich Supercomputing Center for providing the computing time and technical support for the presented work.

[1] A. Sarkar, A. Narváez, and J. Harting. Quantification of the degree of mixing in chaotic micromixers using finite time Lyapunov exponents. *Submitted for publication, arXiv:1012.5549*, 2010.

[2] M. A. Burns. Microfabricated structures for integrated DNA analysis. *Proc. National Acad. Sci. USA*, 68(93):5556–5561, 1996.

[3] P. Watts and S. Haswell. Microfluidic combinatorial chemistry. *Curr. Opin. Chem. Biol.*, 7:380–387, 1996.

[4] V. Hessel, H. Loewe, and F. Schoenfeld. Micromixers- a review on active and passive mixing principles. *Chem. Eng. Sci.*, 60:2479–2501, 2005.

[5] H. Aref. Stirring by chaotic advection. *J. Fluid Mech.*, 143:1–21, 1984.

[6] H. Kim and A. Beskok. Quantification of chaotic strength and mixing in a micro fluidic system. *J. Micromech. Microeng.*, 17:2197–2210, 2007.

[7] F. G. Bessoth, A. de Mello, and A. Manz. Microstructure for effecient conitinuous flow mixing. *Analyt. Comm.*, 36:213–215, 1999.

[8] A. Strook, S. Dertinger, A. Adjari, I. Mezic, H. Stone, and G. Whiteside. Chaotic mixer for microchannels. *Science*, 295:647–651, 2002.

[9] C. Ziemann, L. A. Smith, and J. Kurths. Localized Lyapunov exponents and the prediction of predictability. *Phys. Lett. A*, 4:237–251, 2000.

[10] G. Lapeyre. Characterization of finite-time Lyapunov exponents and vectors in two-dimensional turbulence. *Chaos*, 12(3):688–698, 2002.

[11] T. K. Kang, M. K. Singh, T. H. Kwon, and P. D. Anderson. Chaotic mixing using periodic and aperiodic sequences of mixing protocols. *Microfluids and Nanofluids*, 4(6):589–599, 2007.

[12] S. Succi. *The Lattice Boltzmann Equation for Fluid Dynamics and Beyond*. Oxford University Press, 2001.

[13] Y. H. Qian, D. d'Humieres, and P. Lallemand. Lattice BGK models for Navier-Stokes Equation. *Europhys. Lett.*, 17(6):479–484, 1992.

[14] P. Bhatnagar, E. Gross, and M. Krook. A model for collision process in gases. small amplitude process in charged and neutral one-component systems. *Phys. Rev.*, 94:511–525, 1954.

[15] D. Ruiquiang and L. Jianping. Nonlinear finite-time Lyapunov exponent and predictibility. *Phys. Lett. A*, 364:396–400, 2007.

[16] X. Tang and A. Boozer. Finite time Lyapunov exponent and chaotic advection-diffusion equation. *Physica D*, 95:283–305, 1996.

[17] Y. Lee, C. Shih, P. Tabeling, and C.-M. Ho. Experimental study and non-linear dynamics of time-periodic micro chaotic mixers. *J. Fluid Mech.*, 575:425–448, 2007.

[18] A. Wolf. Determining Lyapnov exponents from a time series. *Physica D*, 16:285–317, 1985.

[19] X. Shan and H. Chen. Lattice Boltzmann model for simulating flows with multiple phases and components. *Phys. Rev. E*, 47(3):1815–1819, 1993.

[20] P. V. Danckewerts. The definition and measurement of some characterisitics of mixtures. *App. Sci. Res.*, 2:279, 1952.

[21] A. D. Stroock and G. J. McGraw. Investigation of the staggered herringbone mixer with a simple analytical model. *Phil. Trans. R. Soc. Lond. A*, 362:923–935, 2004.

[22] H. Shan and G. Doolen. Diffusion in a multicomponent lattic Boltzmann model. *J. Stat. Mech.*, 54:3614, 1996.